arXiv:1103.5977v2 [hep-ph] 1 Jun 2011

Naive time-reversal odd phenomena in semi-inclusive deep-inelastic scattering from light-cone constituent quark models

B. Pasquini[1,2] and P. Schweitzer[3]

[1]*Dipartimento di Fisica Nucleare e Teorica, Università degli Studi di Pavia, Pavia, Italy*
[2]*Istituto Nazionale di Fisica Nucleare, Sezione di Pavia, Pavia, Italy*
[3]*Department of Physics, University of Connecticut, Storrs, CT 06269, USA*

(Dated: March 2011)

We present results for leading-twist azimuthal asymmetries in semi-inclusive lepton-nucleon deep-inelastic scattering due to naively time-reversal odd transverse-momentum dependent parton distribution functions from the light-cone constituent quark model. We carefully discuss the range of applicability of the model, especially with regard to positivity constraints and evolution effects. We find good agreement with available experimental data from COMPASS and HERMES, and present predictions to be tested in forthcoming experiments at Jefferson Lab.

PACS numbers: 13.88.+e, 13.85.Ni, 13.60.-r, 13.85.Qk
Keywords: semi-inclusive deep inelastic scattering, transverse-momentum dependent distribution functions

I. INTRODUCTION

Two out of the 18 structure functions describing the semi-inclusive lepton-nucleon deep-inelastic scattering (SIDIS) process [1, 2], see Fig. 1, are associated at leading order of the hard scale Q with *naively time-reversal odd (T-odd)* transverse-momentum dependent parton distributions (TMDs), the Sivers [3] and Boer-Mulders [4] functions. Their existence is ultimately related to initial and final state interactions in QCD [5] encoded in appropriately defined Wilson lines [6, 7]. T-odd TMDs have unusual "universality" properties, and are predicted to have opposite signs [6] in SIDIS and the Drell-Yan process. The basis for this description is a generalized factorization approach which applies when the final state transverse momentum is small compared to the hard scale [8–10], i.e. $P_{h\perp} \ll Q$ in SIDIS.

Data on the Sivers Boer-Mulders effect from SIDIS are available or forthcoming [11–24] (for a recent review, see Ref. [25]). Both effects were subject to phenomenological studies in SIDIS [26–33] and DY [34–39]. General aspects of the Sivers and Boer-Mulders functions were discussed in [40–43], and quark model calculations were reported in [5, 44–53]. Common to the quark model approaches is that the final (in SIDIS) or initial (in DY) state interactions are modeled by means of a one-gluon exchange (in [52] steps were made to go beyond that).

Among the most recent studies are the calculations in the light-cone constituent quark model (LCCQM) [53]. On the basis of the one-gluon-exchange approximation formulated in the light-cone quantization formalism [54] the Sivers and Boer-Mulders were modeled in [53] using light-cone wave-functions which were previously applied with success to calculations of transversity, electroweak properties of the nucleon, generalized parton distributions, distribution amplitudes [55–57], and T-even leading-twist TMDs [58]. The results illustrate the relevance of different orbital angular momentum components of the nucleon light-cone wave function.

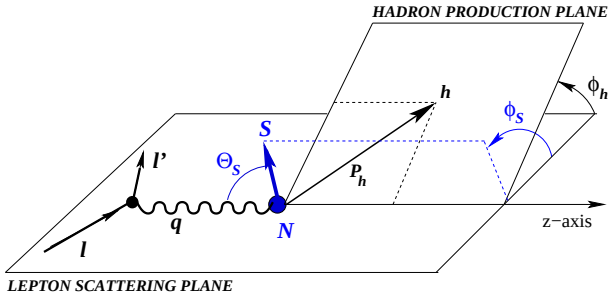

FIG. 1: Kinematics of the SIDIS process $lN \to l'hX$. The azimuthal angles of produced hadron and nucleon polarization vector are ϕ_h and ϕ_S. The transverse momentum of the hadron is $P_{h\perp} \ll Q$ where $Q^2 = -q^2 = (l - l')^2$.

The T-even TMDs from this model [58] were shown to yield results in satisfactory agreement with available SIDIS data [59]. The purpose of this work is to explore whether also the T-odd TMDs from this approach [53] can explain the corresponding SIDIS data. It is important to consider that in contrast to previous studies [55–58], we here probe more than the modeled nucleon light-cone wave-functions. In the present work we moreover also probe to which extent the "one-gluon-exchange approximation" for T-odd TMDs works.

The article is organized as follows. In Sec. II the SIDIS process, and relevant observables are briefly presented. In Sec. III the calculation of the T-odd TMDs [53] is reviewed, positivity and evolution effects are discussed, and limitations of the approach conservatively disclosed. In Secs. IV and V we discuss the numerical results for the asymmetries and compare them to SIDIS data. Conclusions are drawn in Sec. VI. The appendix contains some remarks about the corrections due to the Cahn effect in the $\cos(2\phi_h)$-asymmetry in unpolarized SIDIS.

II. SIVERS AND BOER-MULDERS IN SIDIS

The kinematics of the SIDIS process, the momenta l, l', q, Q^2 and $P_{h\perp} = |\boldsymbol{P}_{h\perp}|$ are defined in Fig. 1. The SIDIS variables are $x = Q^2/(2P\cdot q)$, $y = (P\cdot q)/(P\cdot l)$, and $z = (P\cdot P_h)/(P\cdot q)$ where P is the nucleon momentum. Denoting by σ_0 its spin- and ϕ_h-independent part, the SIDIS cross-section σ (differential in x, y, z and the azimuthal angle ϕ_h which we do not indicate for brevity) can be written as

$$\mathrm{d}^4\sigma = \mathrm{d}^4\sigma_0 \Big\{ 1 + \cos(2\phi_h)\, p_1(y)\, A_{UU}^{\cos(2\phi_h)} + S_T \sin(\phi_h - \phi_S)\, A_{UT}^{\sin(\phi_h-\phi_S)} \ + \ldots \Big\} \quad (1)$$

where $p_1(y) = (1-y)/(1-y+\frac{1}{2}\,y^2)$ up to (systematically neglected) power-suppressed terms, and the dots indicate terms due to T-even TMDs or subleading-twist [60].

$A_{UU}^{\cos(2\phi_h)} = F_{UU}^{\cos(2\phi_h)}/F_{UU}$ and similarly $A_{UT}^{\sin(\phi_h-\phi_S)}$ are the azimuthal asymmetries defined in terms of structure functions. F_{UU} is the unpolarized structure function which gives rise to σ_0. Here the first index U denotes the unpolarized electron beam. The second index U/T refers to the target polarization which can be unpolarized/transverse with respect to the virtual photon (in experiment the transverse target polarization is with respect to the beam, of course, but this is up to power-corrections the same). The superscript reminds us of the kind of angular distribution of the produced hadrons with no index describing an isotropic ϕ_h-distribution. In the Bjorken-limit the relevant structure functions are given at tree-level by [60]

$$F_{UU} = \ \mathcal{C}\Big[\, f_1 D_1 \,\Big], \quad (2)$$

$$F_{UT}^{\sin(\phi_h-\phi_S)} = -\,\mathcal{C}\Big[\frac{\hat{\boldsymbol{h}}\cdot\boldsymbol{p}_T}{M} f_{1T}^{\perp} D_1\Big], \quad (3)$$

$$F_{UU}^{\cos(2\phi_h)} = \mathcal{C}\Big[\frac{2\,(\hat{\boldsymbol{h}}\cdot\boldsymbol{K}_T)\,(\hat{\boldsymbol{h}}\cdot\boldsymbol{p}_T) - \boldsymbol{K}_T\cdot\boldsymbol{p}_T}{z\, m_h M} h_1^{\perp} H_1^{\perp}\Big], \quad (4)$$

where $\hat{\boldsymbol{h}} = \boldsymbol{P}_{h\perp}/P_{h\perp}$ and M (m_h) is the mass of nucleon (produced hadron). The convolutions are defined as

$$\mathcal{C}\Big[\, w\; j\; J\,\Big] = \int \mathrm{d}^2\boldsymbol{p}_T \int \mathrm{d}^2\boldsymbol{K}_T\; \delta^{(2)}(z\,\boldsymbol{p}_T + \boldsymbol{K}_T - \boldsymbol{P}_{h\perp}) \times w(\boldsymbol{p}_T,\, \boldsymbol{K}_T) \sum_a e_a^2\; x\, j^a(x, p_T)\; J^a(z, K_T), \quad (5)$$

with a generic TMD j^a and transverse momentum dependent fragmentation function J^a, and $p_T = |\boldsymbol{p}_T|$ and $K_T = |\boldsymbol{K}_T|$. In Eqs. (2–4) D_1^a is the unpolarized and $H_1^{\perp a}$ the Collins [61, 62] fragmentation function. Notice that in this tree-level treatment one neglects soft factors [8–10].

In order to solve the convolution integrals we will make use of the Gaussian Ansatz. This step could, in principle, be avoided by considering adequately weighted asymmetries [4]. It is given by

$$j^a(x, p_T) = j^a(x)\; \frac{\exp(-p_T^2/\langle p_T^2(j)\rangle)}{\pi\langle p_T^2(j)\rangle}\;,$$
$$J^a(z, K_T) = J^a(z)\; \frac{\exp(-K_T^2/\langle K_T^2(J)\rangle)}{\pi\;\langle K_T^2(J)\rangle}\;. \quad (6)$$

Independently of the model for transverse momenta $F_{UU}(x,z) = \sum_a e_a^2\, x\, f_1^a(x)\, D_1^a(z)$, while with the Ansatz (6) we obtain for the structure functions [59]

$$F_{UT}^{\sin(\phi_h-\phi_S)}(x,z) = -B_0 \sum_a e_a^2\, x\, f_{1T}^{\perp(1)a}(x)\, D_1^a(z), \quad (7)$$

$$F_{UU}^{\cos(2\phi_h)}(x,z) = B_2 \sum_a e_a^2\, x\, h_1^{\perp(1)a}(x) H_1^{\perp(1/2)a}(z), \quad (8)$$

$$B_0 = \frac{z\,\sqrt{\pi}\,M}{\{z^2\,\langle p_T^2(f_{1T}^{\perp})\rangle + \langle K_T^2(D_1)\rangle\}^{1/2}}, \quad (9)$$

$$B_2 = \frac{8\,z\,M\,[\pi\langle K_T^2(H_1^{\perp})\rangle]^{-1/2}}{1 + z^2\langle p_T^2(h_1^{\perp})\rangle\,/\,\langle K_T^2(H_1)\rangle}, \quad (10)$$

with the transverse moments defined as

$$j^{\perp(1)a}(x) = \int \mathrm{d}^2\boldsymbol{p}_T\, \frac{p_T^2}{2M^2}\, j^{\perp a}(x, p_T)\,,$$
$$J^{\perp(1/2)a}(z) = \int \mathrm{d}^2\boldsymbol{K}_T\, \frac{K_T}{2zm_h} J^{\perp a}(z, K_T)\,. \quad (11)$$

The Gaussian Ansatz (6) is for f_1^a and D_1^a phenomenologically well supported for $\langle P_{h\perp}\rangle \ll Q$ [63, 64]. For polarized TMDs it is supported approximately by some models [58, 59, 65, 66]. A rigorous description of p_T-effects would require methods along the QCD-based formalism of [67], as implemented in [68, 69], but for our purposes the Ansatz (6) will be sufficient.

It is important to stress that the description of the SIDIS process in the Bjorken-limit within TMD factorization is generically valid only up to power corrections suppressed by the large scale Q [9, 10]. Typically such corrections do not factorize (TMD factorization beyond leading twist is presently unclear [70] in SIDIS) and must be excluded experimentally by studying the Q-behavior of the observables. In the case of $F_{UU}^{\cos 2\phi_h}$ the parton model provides a way to estimate one of the possible power corrections which is due to the Cahn-effect [71]. This effect gives rise to $\cos\phi_h$ [27, 64] and $\cos(2\phi_h)$ modulations in the unpolarized SIDIS cross section which are suppressed by respectively $\langle p_T(f_1)\rangle/Q$ and $\langle p_T^2(f_1)\rangle/Q^2$. In particular, the latter contributes a power-correction to the Boer-Mulders asymmetry, which is not negligible in the kinematics of present SIDIS experiments [18, 19].

The Cahn-effect and its power correction to $A_{UU}^{\cos(2\phi_h)}$, however, are to a good approximation flavor independent [31, 64]. Below in Sec. V we will therefore consider the difference of the asymmetries for π^- and π^+. Further details are discussed in the Appendix.

III. T-ODD TMDS IN THE LCCQM

In this section we briefly review the calculation of the T-odd TMDs in the light-cone constituent quark model [53]. Within this model, the gauge-link operator entering the quark correlation function which defines the TMDs is approximated by taking into account one-gluon exchange between the struck quark and the spectator quarks in the nucleon described by (real) light-cone wave functions (LCWFs). Working in the light-cone gauge $A^+ = 0$, the T-odd quark TMDs are written in terms of overlap of LCWFs, convoluted with the gluon propagator obtained from the expansion of the gauge link. The final result is of order α_s, which enters as an overall multiplicative factor and is understood at the initial scale μ_0 of the model.

The value of $\alpha_s(\mu_0)$ was fixed by determining the initial model scale μ_0 following [72] as follows. Since the model has only valence quark degrees of freedom, one requires μ_0 to be such that evolving the (total in the model) momentum fraction carried by valence quarks, $\langle x(\mu_0)\rangle_V = \sum_q \int \mathrm{d}x\, x(f_1^q - f_1^{\bar{q}})(x,\mu_0) = 1$, from μ_0 to experimentally relevant scales one matches the NLO phenomenological value $\langle x(Q)\rangle_V = 0.36$ at $Q^2 = 10\,\mathrm{GeV}^2$ [73]. In previous works μ_0 was tuned to reproduce exactly the phenomenological value of $\langle x(Q)\rangle_V$. Here we content ourselves with reproducing it within 10 %, which is acceptable in view of the generic model accuracy of (10–30) % [59]. Allowing for a 10 %-overestimate of $\langle x(Q)\rangle_V$ yields a higher μ_0 and smaller $\alpha_s(\mu_0)$, and better convergence. The evolution was performed in the variable flavor-number scheme with heavy-quark mass thresholds $m_c = 1.4$ GeV, $m_b = 4.75$ GeV, $m_t = 175$ GeV with $\alpha_s^{\mathrm{NLO}}(M_Z^2) = 0.12018$ at next-to-leading order (NLO, $\overline{\mathrm{MS}}$ scheme) from [73]. We obtain for the initial model scale

$$\mu_0^{\mathrm{NLO}} = 508\,\mathrm{MeV}, \quad \frac{\alpha_s^{\mathrm{NLO}}(\mu_0^2)}{4\pi} = 0.128 \qquad (12)$$

(notice that $\Lambda_{\mathrm{NLO}}^{(3,4,5)} = 402$, 341, 239 MeV in [73]). The strategy of fixing the model scale is basically the same as in previous works. Here we introduced the variable flavor number scheme, and updated the value of $\alpha_s(M_Z^2)$. As a result, we find a higher value for the hadronic scale of the model, corresponding to a somewhat smaller coupling compared to [53]. For the calculations of T-odd TMDs, we will adopt the value of α_s in Eq. (12).

The LCWF of the nucleon is modeled as described in [53, 58]. In particular, to disentangle the spin-spin and spin-orbit quark correlations encoded in the TMDs, we expand the three-quark LCWF in a basis of eigenstates of orbital angular momentum, which yields 6 independent amplitudes corresponding to different combinations of quark helicity and orbital angular momentum [75].

Assuming SU(6) symmetry, these light-cone amplitudes have a particularly simple structure, with spin and isospin dependence factorized from a momentum-dependent function with spherical symmetry. Under this assumption the orbital angular momentum content of the wave function is fully generated by the Melosh rotations which boost the rest-frame (canonical) spin of the quarks into light-cone helicities. For the momentum-dependent part of the LCWF we adopt the phenomenological description with parameters fitted to hadronic structure constants from [76] which gave satisfactory results in previous works [56–59].

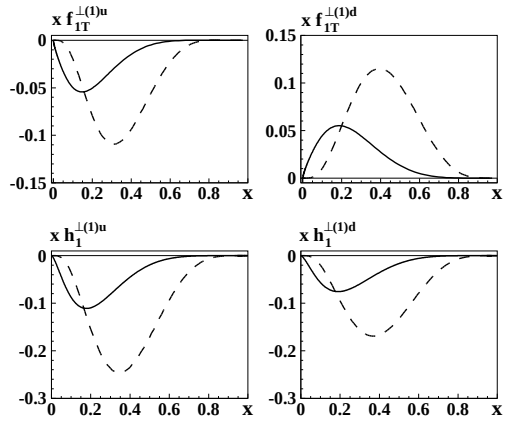

FIG. 2: Transverse moments $f_{1T}^{\perp(1)q}(x)$ and $h_1^{\perp(1)q}(x)$ in a proton for up (left) and down (right) quark, as function of x. The dashed curves show the results at the hadronic scale μ_0 of the model . The solid curves correspond to the results after LO evolution to $Q^2 = 2.5$ GeV^2, using the evolution patterns of the unpolarized parton distribution (transversity) for the Sivers (Boer-Mulders) function.

The results for the (1)-moments of the Sivers and Boer-Mulders functions as defined in (11) are shown in Fig. 2. The dashed curves show the results at the hadronic scale of the model, while the solid curves are obtained by applying LO evolution to $Q^2 = 2.5$ GeV^2 [77]. Since the exact evolution equations for the T-odd TMDs are still under study [78–81, 83], we use those evolution equations which seem most promising to "simulate" the correct evolution.

The chiral-even Sivers function is evolved according to the LO *non-singlet* evolution pattern of $f_1^a(x)$, which has the advantage of preserving the Burkardt sum rule [42]. This non-trivial constraint for model calculations is satisfied in the LCCQM at the initial model scale [53]. For the chiral-odd Boer-Mulders function we use the evolution pattern of $h_1^q(x)$. The so evolved model results are consistent with the first extractions [26–31] concerning signs and magnitudes of the various flavors, and the positions of their maxima in x.

As can be seen in Fig. 2, evolution effects are important, and this raises the question how reliably we estimated them here. The exact answer to this question will be given after the TMD-evolution formalism discussed in [69] for $f_1^a(x, p_T)$ has been generalized to include the Sivers and Boer-Mulders effects. Until then, we can try to gain some intuition by investigating how much the results would change if we used different ways of simulat-

ing the evolution effects for T-odd TMDs. For that we explored also alternative evolution patterns, and found that the corresponding results vary within (10–20) %. This indicates that the theoretical uncertainty associated with evolution effects is not larger than the model accuracy [82]. An interesting result is that the model supports approximately the Gaussian Ansatz, both for T-odd [53] and T-even [59] TMDs.

A point deserving particular attention are inequalities among twist-2 TMDs [40], which can be written as

$$\mathcal{P}^q_{\rm Siv}(x,p_T) \equiv f_1^q(x,p_T)^2 - g_1^q(x,p_T)^2 - \frac{p_T^2}{M_N^2}\, g_{1T}^{\perp q}(x,p_T)^2 - \frac{p_T^2}{M_N^2}\, f_{1T}^{\perp q}(x,p_T)^2 \geq 0\,, \quad (13)$$

$$\mathcal{P}^q_{\rm BM}(x,p_T) \equiv f_1^q(x,p_T)^2 - g_1^q(x,p_T)^2 - \frac{p_T^2}{M_N^2}\, h_{1L}^{\perp q}(x,p_T)^2 - \frac{p_T^2}{M_N^2}\, h_1^{\perp q}(x,p_T)^2 \geq 0\,. \quad (14)$$

In a consistent model framework the inequalities (13)-(14) should hold. However, as observed in [50], for certain values of x and p_T numerous models violate already the weaker inequalities $\frac{p_T}{M_N}\,|f_{1T}^{\perp q}(x,p_T)| \leq f_1^q(x,p_T)$, and $\frac{p_T}{M_N}\,|h_1^{\perp q}(x,p_T)| \leq f_1^q(x,p_T)$ following from (13), (14).

The reason is apparent. The calculations of T-odd TMDs are within the given models correct. But while T-odd TMDs are evaluated to $\mathcal{O}(\alpha_s)$, the "expansion" of T-even TMDs is truncated in the quark models at $\mathcal{O}(\alpha_s^0)$. In order to preserve unitarity, and hence the inequalities, one should evaluate also T-even TMDs consistently to order $\mathcal{O}(\alpha_s)$. To best of our knowledge, this has so far not been done in any model, and would also go beyond the scope of the present work.

Having established that one cannot expect the inequalities (13, 14) to be satisfied in our approach either, let us see for which values of x and p_T they are violated. For that, in Fig. 3 we plot $\mathcal{P}^q_{\rm Siv,BM}(x,p_T)$, Eqs. (13, 14), vs. p_T^2 for selected values of $x = 0.2,\, 0.3,\, 0.4$ at the low model scale. $\mathcal{P}^q_{\rm Siv,BM}(x,p_T)$ should be always positive, and we see that this condition is violated only at small x and for p_T^2 significantly larger than the respective $\langle p_T^2\rangle$. Now it is important to recall several facts. First, quark models do not describe reliably small x. Notice that the region of $x \lesssim 0.2$ at the low model scale corresponds after (correct or approximate) evolution to $x \lesssim \mathcal{O}(10^{-2})$. Thus, practical consequences (if any) of the violation of inequalities are beyond the region of x where quark models can be applied. Second, in the following we will restrict ourselves to the use of p_T-integrated results for the (1)-moments, and those are dominated by the regions of p_T of the order of magnitude of $\langle p_T^2\rangle$ and smaller, i.e. where the inequalities are satisfied.

To conclude, though we have to admit that the model predictions do not satisfy the inequalities for all x and p_T, we can be assured that — in the way we will use them for phenomenological calculations — this will not yield any artifacts. In this sense we will consider our results as compliant with positivity constraints.

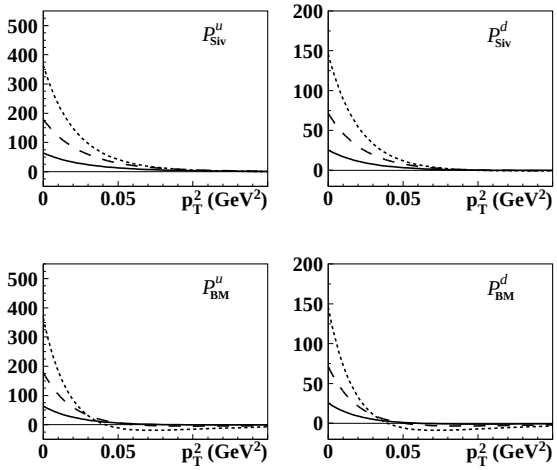

FIG. 3: The positivity relations involving the Sivers (upper panels) and Boer-Mulders functions (lower panels) from Eqs. (13) and (14), respectively, as function of p_T^2 at different values of x: $x = 0.3$ (short-dashed curves), $x = 0.4$ (long-dashed curves), and $x = 0.5$ (solid curves). The left (right) panels show the results for up (down) quark.

IV. SIVERS ASYMMETRY

In this Section we discuss the asymmetry $A_{UT}^{\sin(\phi_h-\phi_S)}$ due to the Sivers effect. With the model results referring to a low scale, it is not only necessary to evolve the Sivers function in x, but also to account for p_T-broadening [67] (all this applies equally to the Boer-Mulders function). In principle, one could feed the Collins-Soper-Sterman (CSS) equation [67] with the model results as initial conditions. We refrain from this step, because the CSS formalism is not yet developed for cases including polarization effects, while in the unpolarized case the result is known: one would expect to reproduce, within model accuracy, the phenomenological value $\langle p_T^2(f_1)\rangle \sim 0.4\,{\rm GeV}^2$ at HERMES energies. Therefore we proceed as follows.

We assume that the Gaussian shape is approximately preserved through the CSS evolution but the Gaussian widths increase with energy [64, 69], and we assume that to lowest order approximation this p_T-broadening is polarization independent. We use the model predictions for $f_{1T}^{\perp(1)q}(x)$ (approximately evolved in x as discussed in Sec. III) which are presumably less affected by Sudakov effects [84] than $f_{1T}^{\perp q}(x)$ with which one also could work within the Gauss model. In the expression (7) for the Sivers asymmetry we use $\langle K_T^2(D_1)\rangle = 0.16\,{\rm GeV}^2$ [64] and the Gaussian width of the Sivers function, which is $\langle p_T^2(f_{1T}^\perp)\rangle \approx 0.9\,\langle p_T^2(f_1)\rangle$ in the model [53]. According to our assumption one may expect this prediction to be roughly valid also at experimentally relevant scales, because to lowest order approximation p_T-broadening effects are polarization-independent. In [59] positive experience was made with such estimates of p_T-broadening effects. Further studies are required for more precision.

In the numerator of the Sivers asymmetry we use

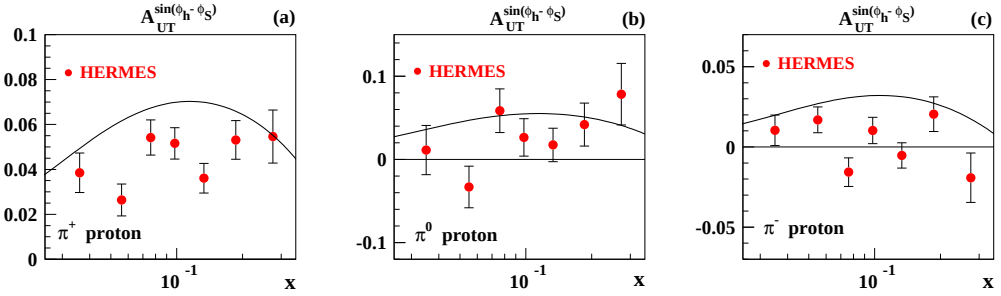

FIG. 4: The single-spin asymmetry $A_{UT}^{\sin(\phi_h-\phi_S)}$ for pion production off proton in SIDIS, as function of x. The HERMES data are from [15]. The theoretical curves are obtained on the basis of the LCCQM predictions for $f_{1T}^{\perp(1)q}(x)$ [53].

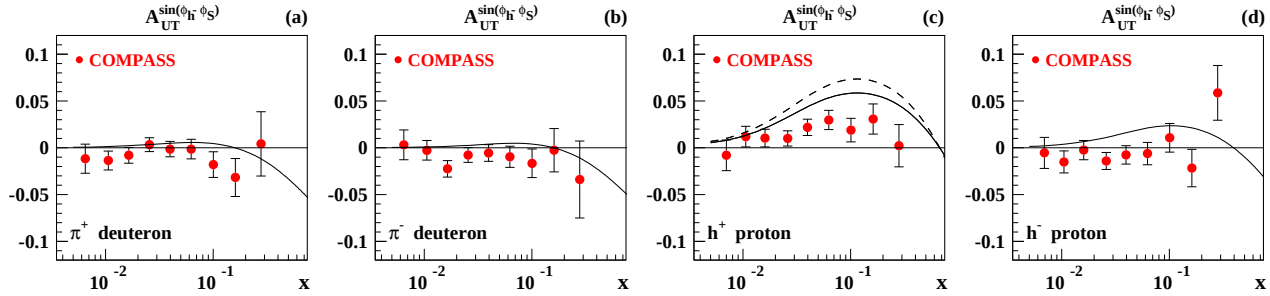

FIG. 5: $A_{UT}^{\sin(\phi_h-\phi_S)}$ for charged pion (hadron) production off deuteron (proton) in SIDIS, as function of x. The COMPASS data are from [13, 14]. The theoretical curves are obtained on the basis of the LCCQM predictions for $f_{1T}^{\perp(1)q}(x)$ [53]. The dotted curve in panel (c) shows the results without the effects of p_T-broadening (see text).

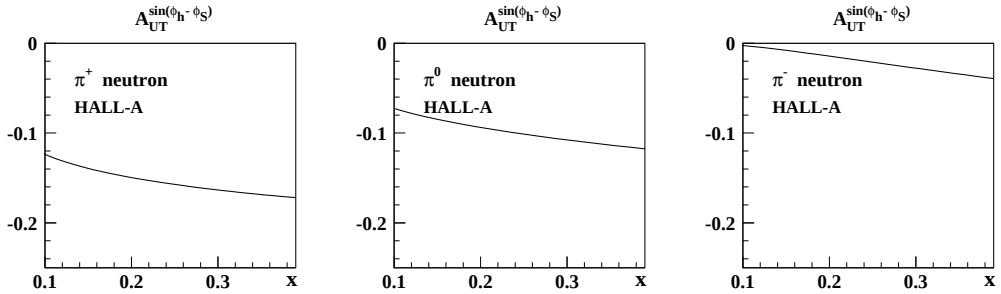

FIG. 6: $A_{UT}^{\sin(\phi_h-\phi_S)}$ for pion production off neutron in SIDIS, as function of x. The theoretical predictions are obtained on the basis of results for $f_{1T}^{\perp(1)q}(x)$ from LCCQM [53] for the kinematics of the Hall-A experiment at Jefferson Lab [22].

model predictions for $f_1^a(x)$ LO-evolved to a scale of $2.5\,\mathrm{GeV}^2$. For $D_1^a(z)$ we use the LO parameterization from [85] at the same scale.

In this way we obtain in the kinematics of the HERMES experiment, $\langle Q^2\rangle \approx 2.5\,\mathrm{GeV}^2$ and $0.2 < z < 0.7$, the results for the x-dependence of the Sivers asymmetry for pion production off a proton target shown in Fig. 4. Keeping in mind that the quark model approach is not expected to be reliable in the small-x region, we observe a good description of the data within the accuracy of our approach. (Due to the absence of sea quarks in our approach the Sivers asymmetries for kaons would be very similar to the pion asymmetries. The explanation of a possible difference in π^+ and K^+ Sivers asymmetries [15] is beyond the scope of our approach.)

Next we discuss the COMPASS data which have $\langle Q^2\rangle$ similar to HERMES and $0.2 < z < 1$, but were measured at a significantly higher $s = (P+l)^2 \approx 2M_N E_{\mathrm{beam}}$ with $E_{\mathrm{beam}} = 160\,\mathrm{GeV}$ (vs. $E_{\mathrm{beam}} = 27\,\mathrm{GeV}$ at HERMES). From Drell-Yan it is known that at higher energies the TMDs tend to be broader [64] as follows from the CSS formalism [67, 69]. There are indications that this is also the case in SIDIS [64], namely one has $\langle P_{h\perp}^2\rangle = 0.27\,\mathrm{GeV}^2$ at HERMES [88] to be compared with $\langle P_{h\perp}^2\rangle = 0.41\,\mathrm{GeV}^2$ at COMPASS [89]. Both results refer to a common $z \sim 0.55$ but different $\langle x\rangle$. If we assume an x-independent Gaussian width of f_1^a (the data are compatible with this assumption [64]), the observed

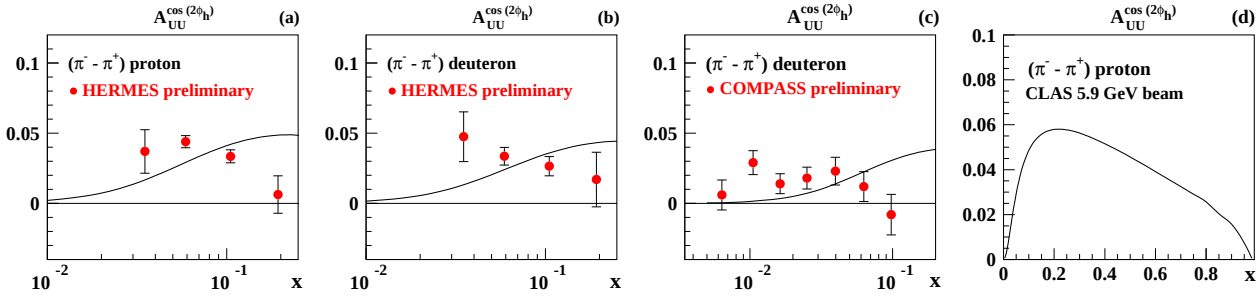

FIG. 7: The difference of azimuthal asymmetries $A_{UU}^{\cos(2\phi_h)}$ for negative and positive pions or hadrons, as function of x. The experimental points were obtained taking the differences of preliminary π^- and π^+ HERMES data [18], and preliminary h^- and h^+ COMPASS data [19]. The error bars show the propagation of statistical errors, and do not include systematic errors. The theoretical curves are obtained using $h_1^{\perp(1)q}(x)$ from the LCCQM [53]. Panel (d) shows a prediction for Jefferson Lab.

broadening of $\langle P_{h\perp}^2\rangle = \langle K_T^2(D_1)\rangle + z^2\langle p_T^2(f_1)\rangle$ has to be attributed to broadenings of the Gaussian widths of f_1^a and D_1^a. In order to crudely estimate these effects we assume that at COMPASS the widths of f_1^a and D_1^a are equally broadened compared to HERMES as follows

$$\langle p_T^2(f_1)\rangle_{\rm COMPASS} = \langle p_T^2(f_1)\rangle_{\rm HERMES} + \delta\langle\kappa_T^2\rangle\ ,$$
$$\langle K_T^2(D_1)\rangle_{\rm COMPASS} = \langle K_T^2(f_1)\rangle_{\rm HERMES} + \delta\langle\kappa_T^2\rangle\ , \quad (15)$$

with $\delta\langle\kappa_T^2\rangle \approx 0.11\,{\rm GeV}^2$ needed to explain the larger $\langle P_{h\perp}^2\rangle$ at COMPASS. This change in parameters also affects (broadens) the Gaussian width of the Sivers function (estimated here as $\langle p_T^2(f_{1T}^\perp)\rangle \approx 0.9\,\langle p_T^2(f_1)\rangle$, see above). In this way we obtain the results shown in Fig. 5.

We observe a good agreement of the model results with the COMPASS data on the Sivers effect in $\pi^\pm$ production from a deuteron target [13] in Figs. 5a, b, and charged hadron production from a proton target [14] in Figs. 5c, d. (For simplicity we approximated the results for charged hadrons by charged pions, which account for about 90 % of charged hadrons at COMPASS energies.)

Notice that, had we neglected the p_T-broadening at COMPASS as compared to HERMES, the model would have clearly overestimated π^+ data from proton at COMPASS, see Fig. 5c. Indeed, Fig. 5c seems to indicate that the p_T-broadening could even be somewhat stronger than estimated on the basis of (15). In Figs. 5a, b, d the neglect of broadening effects would be less significant, or completely within error bars.

Finally, we present predictions for a forthcoming Hall-A experiment at Jefferson Lab [21] with a 5.9 GeV beam. Here s is sufficiently close to HERMES, such that it is not necessary to account for p_T-broadening effects, in contrast to COMPASS, Eq. (15) [64]. In this experiment $\langle Q^2\rangle \sim 2\,{\rm GeV}^2$ and $0.42 < z < 0.66$. The results for this kinematics are shown in Fig. 6. At Hall-A the asymmetry is larger because roughly $B_0(z) \propto z$ in (7) and Hall-A probes larger z compared to HERMES and COMPASS.

To summarize, we find that our model framework provides a satisfactory description of the SIDIS data on the Sivers effect from HERMES and COMPASS [13–15]. Future data from Jefferson Lab will allow further tests.

V. BOER-MULDERS ASYMMETRY

In this section we focus on the asymmetry $A_{UU}^{\cos(2\phi_h)}$ due to the Boer-Mulders effect. The asymmetry (8) is calculated similarly to the Sivers asymmetry in Sec. IV.

We use the model predictions for $h_1^{\perp(1)q}(x)$ from [53]. For the Collins function and its Gaussian width we use the information from [86, 87], and for the width of the Boer-Mulders function we use the LCCQM model prediction $\langle p_T^2(h_1^\perp)\rangle \approx 0.95\,\langle p_T^2(f_1)\rangle$ [53], which we again assume to be approximately valid at experimentally relevant scales. For $f_1^a(x)$ in the numerator of the asymmetry we use the model predictions LO-evolved to $2.5\,{\rm GeV}^2$ [90], and for $D_1^a(z)$ the LO parameterization from [85] at the same scale. The p_T-broadening effects at the higher energies in the COMPASS as compared to HERMES, are estimated similarly to Sec. IV i.e. we use the HERMES value $\langle K_T^2(H_1^\perp)\rangle \approx 0.25\langle K_T^2(D_1)\rangle$ from [87], and consider p_T-broadening analog to Eq. (15).

As discussed in detail in Sec. II, the Cahn-effect [71] generates an $1/Q^2$ power-correction to the $\cos(2\phi_h)$ modulation in the unpolarized SIDIS cross section which cannot be neglected in the kinematics of the HERMES or COMPASS experiments [31, 64]. In principle, one can try to model this power-correction [31]. For that one could use the updated phenomenological results for $\langle p_T^2(f_1)\rangle$ and $\langle K_T^2(D_1)\rangle$ [64] which are sufficient to determine the Cahn-effect. Alternatively, one could explore data on the $\cos(2\phi_h)$-asymmetry of neutral pions, where due to the flavor-dependence of the Collins function [86, 87] the leading-twist Boer-Mulders effect largely cancels, see Appendix. In any case, this step constitutes an *additional* modeling step (of a non-factorizable twist-4 contribution), and we prefer to avoid it.

However, the Cahn effect contamination in $A_{UU}^{\cos(2\phi_h)}$ is flavor-independent to a good approximation, and largely cancels out in differences of π^- and π^+ asymmetries. Such differences can be determined from the preliminary data [18, 19] and we shall confront our model results with them instead. The results are shown in Figs. 7a-c. (We again approximate at COMPASS $h^\pm$ results by $\pi^\pm$.)

Again it is important to recall that the quark results should not be expected to be reliable in the small-x region. In the region of $x \sim 0.1$ the model describes well the size of the asymmetry differences, but it seems not to follow the trend of the data at larger $x \gtrsim 0.2$. However, one has to keep in mind the preliminary status of the data [18, 19]. Moreover, considering systematic errors of the data which are not included in Figs. 7a-c, the discrepancy could be well within model accuracy.

From the available Jefferson Lab data [16, 17] the difference of π^- and π^+ $\cos(2\phi_h)$-asymmetries cannot be accessed, but forthcoming CLAS data will allow that [20]. In the CLAS experiment we have $\langle Q^2 \rangle \sim 1.9\,\mathrm{GeV}^2$ with $0.1 < x < 0.6$ and $0.4 < z < 0.7$. The predictions for this kinematics are shown in Fig. 7d. Since the x values of the CLAS experiment cover the region dominated by the valence-quark contribution, these data will provide an important test of the model.

To summarize, our approach is compatible with preliminary data from COMPASS and HERMES. Further insights can be expected from Jefferson Lab, before [20] and after the 12 GeV beam energy upgrade [23], and on long term from the future Electron-Ion Collider [24].

VI. CONCLUSIONS

In this work we have studied the leading-twist azimuthal asymmetries in SIDIS due to T-odd TMDs on the basis of predictions from the light-cone constituent-quark model [53]. Since the model results refer at a low hadronic scale, we discussed how to take into account the effects of the evolution for the description of data referring to high scales of typically several GeV^2. We tackled this issue in two steps. First, for the p_T-dependence of the distributions we employed the Gaussian Ansatz and expressed the asymmetries in terms of (1)-transverse moments of TMDs. The Gaussian widths of the distributions were assumed x-independent, which is supported by phenomenology, and p_T-broadening effects were estimated. In the second step, we evolved the transverse moments of TMDs to experimental scales by employing those evolution equations which seem most promising to simulate the correct evolution. For the Sivers distribution we used the non-singlet evolution pattern of $f_1^a(x)$. This allows to preserve the Burkardt sum rule — valid at the initial scale of the model [53] — also at higher scales. For the chiral-odd Boer-Mulders function we used the evolution pattern of transversity.

We obtained a good description of the Sivers asymmetry, and satisfactory results for the Boer-Mulders asymmetry in comparison with available experimental data from HERMES and COMPASS. In the case of the Boer-Mulders asymmetry we considered differences of asymmetries for π^- and π^+ to avoid the modeling of twist-4 power corrections ('Cahn effect'). Furthermore, we presented model predictions for forthcoming experiments at Jefferson Lab, which will extend the available data far into the valence-x region where the model is expected to work best, and provide an important test of its dynamics.

Our results indicate that the use of the one-gluon-exchange-mechanism to model T-odd TMDs (as implemented in [53]) yields phenemenologically reasonable results, although a truncation of the expansion of the gauge-link at $\mathcal{O}(\alpha_s)$ seems not a priori justifiable.

The present work completes the study in Ref. [59] where leading-twist spin asymmetries due to T-even TMDs were calculated. We observe that the light-cone constituent-quark model, based on overlap representation of TMDs in terms of light-cone wave functions, provides a good description of intrinsic transverse parton momentum effects in the range of applicability of the model.

Acknowledgements. We thank M. Contalbrigo from the HERMES collaboration, and E. Kabuss, A. Martin and G. Sbrizzai from the COMPASS collaboration for making available the (final and preliminary) data. We also acknowledge helpful discussions with A. V. Efremov, W. Gohn, J.-F. Rajotte, T. Rogers and F. Yuan. B. P. is grateful for the hospitality to the Department of Physics of the University of Connecticut where this work was initiated. The work was supported in part by DOE contract DE-AC05-06OR23177, under which Jefferson Science Associates, LLC, operates the Jefferson Lab, by the Research Infrastructure Integrating Activity "Study of Strongly Interacting Matter" (acronym HadronPhysics2, Grant Agreement n. 227431) under the Seventh Framework Programme of the European Community, and by the Italian MIUR through the PRIN 2008EKLACK "Structure of the nucleon: transverse momentum, transverse spin and orbital angular momentum".

Appendix A: Remark on Cahn effect

Finally, a remark is in order on $A_{UU}^{\cos(2\phi_h)}$ for definite pions, where the Cahn effect $1/Q^2$-correction cannot be neglected [31, 64] though it could be small in largest x-bins at COMPASS. In principle, one may model this contribution [31] with due care to the energy dependence of the Gauss parameters [64, 69]. However the problem remains how to test independently such an additional modeling of a presumably non-factorizing twist-4 term. We are not aware of a 'rigorous procedure', but the following observation may turn out helpful. The favored ($u \to \pi^+$) and unfavored ($u \to \pi^-$) Collins fragmentation functions are similar in magnitude but have opposite signs [86, 87].

In the $A_{UT}^{\sin(\phi_h+\phi_S)}$ asymmetry for π^0 (which is due to the Collins effect and potentially not or less affected by power-corrections) this yields nearly exact flavor cancellations, as seen in data [91]. Since this is a property of the Collins function, one expects the Collins effect to also

cancel out in the π^0 $\cos(2\phi_h)$-asymmetry, i.e.

$$A_{UU}^{\cos(2\phi_h)}(\pi^0) \approx A_{UU,\,\mathrm{Cahn}}^{\cos(2\phi_h)} < 0\,, \qquad \text{(A1)}$$

where $A_{UU,\,\mathrm{Cahn}}^{\cos(2\phi_h)}$ is the Cahn effect contribution, which is negative [71] and largely flavor independent [31, 64]. This would then mean that

$$A_{UU}^{\cos(2\phi_h)}(\pi^+) \approx A_{UU}^{\cos(2\phi_h)}(\pi^+)_{\mathrm{BM}} + A_{UU,\,\mathrm{Cahn}}^{\cos(2\phi_h)}\,, \quad \text{(A2)}$$

$$A_{UU}^{\cos(2\phi_h)}(\pi^-) \approx A_{UU}^{\cos(2\phi_h)}(\pi^-)_{\mathrm{BM}} + A_{UU,\,\mathrm{Cahn}}^{\cos(2\phi_h)}\,. \quad \text{(A3)}$$

This is not to be confused with relations due to isospin invariance, which allow one to express π^0 cross sections in terms of $\pi^\pm$ cross sections (i.e. which connect the numerators *or* the denominators of the asymmetries). Eqs. (A1)-(A3) indicate how to model the Cahn-effect in a given experiment. This might be a more reliable procedure than using other sources of information. The procedure can be iteratively improved to take into account flavor-dependencies in the Cahn-effect and non-exact cancellations of the Collins effect in the neutral pion $\cos(2\phi_h)$-asymmetry. In particular, Eqs. (A2) and (A3) show our underlying assumption in Sec. V that in the difference of charged pion $\cos(2\phi_h)$-asymmetries the Cahn effect largely cancels out.

[1] A. Kotzinian, Nucl. Phys. B **441**, 234 (1995).
[2] P. J. Mulders and R. D. Tangerman, Nucl. Phys. B **461**, 197 (1996) [Erratum-ibid. B **484** (1997) 538].
[3] D. W. Sivers, Phys. Rev. D **41**, 83 (1990); Phys. Rev. D **43**, 261 (1991).
[4] D. Boer and P. J. Mulders, Phys. Rev. D **57**, 5780 (1998).
[5] S. J. Brodsky, D. S. Hwang and I. Schmidt, Phys. Lett. B **530**, 99 (2002); Nucl. Phys. B **642**, 344 (2002).
[6] J. C. Collins, Phys. Lett. B **536**, 43 (2002).
[7] A. V. Belitsky, X. Ji and F. Yuan, Nucl. Phys. B **656**, 165 (2003); X. D. Ji and F. Yuan, Phys. Lett. B **543**, 66 (2002); D. Boer, P. J. Mulders and F. Pijlman, Nucl. Phys. B **667**, 201 (2003).
[8] J. C. Collins and D. E. Soper, Nucl. Phys. B **193**, 381 (1981) [Erratum-ibid. B **213**, 545 (1983)].
[9] X. D. Ji, J. P. Ma and F. Yuan, Phys. Rev. D **71**, 034005 (2005); Phys. Lett. B **597**, 299 (2004).
[10] J. C. Collins and A. Metz, Phys. Rev. Lett. **93**, 252001 (2004).
[11] A. Airapetian *et al.* [HERMES Collaboration], Phys. Rev. Lett. **94**, 012002 (2005).
[12] V. Y. Alexakhin *et al.* [COMPASS Collaboration], Phys. Rev. Lett. **94**, 202002 (2005). E. S. Ageev *et al.* [COMPASS Collaboration], Nucl. Phys. B **765**, 31 (2007).
[13] M. Alekseev *et al.* [COMPASS Collaboration], Phys. Lett. B **673**, 127 (2009).
[14] M. G. Alekseev *et al.* [COMPASS Collaboration], Phys. Lett. B **692**, 240 (2010).
[15] A. Airapetian *et al.* [HERMES Collaboration], Phys. Rev. Lett. **103**, 152002 (2009).
[16] H. Mkrtchyan, P. E. Bosted *et al.*, Phys. Lett. **B665**, 20 (2008); R. Asaturyan, R. Ent, H. Mkrtchyan, T. Navasardyan, V. Tadevosyan *et al.*, arXiv:1103.1649 [nucl-ex].
[17] M. Osipenko *et al.* [CLAS Collaboration], Phys. Rev. **D80**, 032004 (2009).
[18] F. Giordano and R. Lamb, arXiv:1011.5422 [hep-ex].
[19] G. Sbrizzai [COMPASS Coll.], arXiv:1012.4910 [hep-ex].
[20] W. Gohn, H. Avakian, K. Joo, M. Ungaro, AIP Conf. Proc. **1149**, 461 (2009).
[21] X. Jiang, J.-P. Chen, J.-C. Peng, H. Gao, E. Cisbani, Hall A Transversity Experiment E-06-010/E-06-011.
[22] H. Gao *et al.*, Eur. Phys. J. Plus **126**, 1-16 (2011).
[23] H. Avakian *et al.*, JLab Experiment PR-09-008 (2008).
[24] M. Anselmino, H. Avakian, D. Boer, F. Bradamante, M. Burkardt, J. P. Chen, E. Cisbani, M. Contalbrigo *et al.*, Eur. Phys. J. **A47**, 35 (2011).
[25] V. Barone, F. Bradamante and A. Martin, Prog. Part. Nucl. Phys. **65**, 267 (2010).
[26] A. V. Efremov, K. Goeke, S. Menzel, A. Metz and P. Schweitzer, Phys. Lett. B **612**, 233 (2005).
[27] M. Anselmino *et al.*, Phys. Rev. D **71**, 074006 (2005).
[28] W. Vogelsang and F. Yuan, Phys. Rev. D **72**, 054028 (2005).
[29] J. C. Collins *et al.*, Phys. Rev. D **73**, 014021 (2006). S. Arnold *et al.*, arXiv:0805.2137 [hep-ph].
[30] M. Anselmino *et al.*, Eur. Phys. J. A **39** (2009) 89.
[31] V. Barone, S. Melis and A. Prokudin, Phys. Rev. D **81**, 114026 (2010).
[32] V. Barone, Z. Lu and B. Q. Ma, Phys. Lett. B **632**, 277 (2006); Eur. Phys. J. C **49**, 967 (2007). V. Barone, A. Prokudin and B. Q. Ma, Phys. Rev. D **78**, 045022 (2008). B. Zhang, Z. Lu, B. Q. Ma and I. Schmidt, Phys. Rev. D **78**, 034035 (2008).
[33] A. Bacchetta, M. Radici, F. Conti and M. Guagnelli, Eur. Phys. J. A **45**, 373 (2010).
[34] D. Boer, Phys. Rev. D **60**, 014012 (1999).
[35] J. C. Collins *et al.*, Phys. Rev. D **73**, 094023 (2006). M. Anselmino *et al.*, Phys. Rev. D **79**, 054010 (2009).
[36] A. Bianconi and M. Radici, Phys. Rev. D **73**, 034018 (2006); Phys. Rev. D **73**, 114002 (2006).
[37] A. Sissakian *et al.*, Eur. Phys. J. C **59**, 659 (2009); Phys. Rev. D **72**, 054027 (2005).
[38] Z. B. Kang and J. W. Qiu, Phys. Rev. D **81**, 054020 (2010).
[39] Z. Lu and I. Schmidt, Phys. Rev. D **81**, 034023 (2010).
[40] A. Bacchetta, M. Boglione, A. Henneman and P. J. Mulders, Phys. Rev. Lett. **85**, 712 (2000).
[41] P. V. Pobylitsa, arXiv:hep-ph/0301236.
[42] M. Burkardt, Phys. Rev. D **69** (2004) 091501(R); Phys. Rev. D **69** (2004) 057501 .
[43] S. J. Brodsky and F. Yuan, Phys. Rev. D **74**, 094018 (2006).
[44] F. Yuan, Phys. Lett. B **575**, 45 (2003).
[45] L. P. Gamberg, G. R. Goldstein and K. A. Oganessyan, Phys. Rev. D **67**, 071504 (2003). L. P. Gamberg and G. R. Goldstein, Phys. Lett. B **650**, 362 (2007).
[46] S. Meissner, A. Metz and K. Goeke, Phys. Rev. D **76**,

034002 (2007).
[47] L. P. Gamberg, G. R. Goldstein and M. Schlegel, Phys. Rev. D **77**, 094016 (2008); arXiv:0708.2580 [hep-ph].
[48] A. Courtoy, F. Fratini, S. Scopetta and V. Vento, Phys. Rev. D **78**, 034002 (2008). A. Courtoy, S. Scopetta and V. Vento, Phys. Rev. D **80**, 074032 (2009).
[49] A. Bacchetta, F. Conti and M. Radici, Phys. Rev. D **78**, 074010 (2008).
[50] A. Kotzinian, arXiv:0806.3804 [hep-ph].
[51] J. R. Ellis, D. S. Hwang, A. Kotzinian, Phys. Rev. **D80**, 074033 (2009).
[52] L. Gamberg and M. Schlegel, Phys. Lett. B **685**, 95 (2010); arXiv:1012.3395 [hep-ph].
[53] B. Pasquini and F. Yuan, Phys. Rev. D **81**, 114013 (2010).
[54] S. J. Brodsky, B. Pasquini, B. W. Xiao and F. Yuan, Phys. Lett. B **687**, 327 (2010).
[55] B. Pasquini, M. Pincetti and S. Boffi, Phys. Rev. D **72**, 094029 (2005); Phys. Rev. D **76**, 034020 (2007).
[56] B. Pasquini, and S. Boffi, Phys. Rev. D **76**, 074011 (2007); Riv. Nuovo Cim. **30**, 387 (2007).
[57] B. Pasquini, M. Pincetti and S. Boffi, Phys. Rev. D **80**, 014017 (2009).
[58] B. Pasquini, S. Cazzaniga and S. Boffi, Phys. Rev. D **78**, 03425 (2008).
[59] S. Boffi, A. V. Efremov, B. Pasquini, P. Schweitzer, Phys. Rev. D **79**, 094012 (2009).
[60] A. Bacchetta, M. Diehl, K. Goeke, A. Metz, P. J. Mulders and M. Schlegel, JHEP **0702**, 093 (2007).
[61] A. V. Efremov, L. Mankiewicz and N. A. Tornqvist, Phys. Lett. B **284**, 394 (1992).
[62] J. C. Collins, Nucl. Phys. B **396**, 161 (1993).
[63] U. D'Alesio and F. Murgia, Phys. Rev. D **70**, 074009 (2004).
[64] P. Schweitzer, T. Teckentrup and A. Metz, Phys. Rev. D **81**, 094019 (2010).
[65] H. Avakian, A. V. Efremov, P. Schweitzer and F. Yuan, Phys. Rev. D **81**, 074035 (2010); Phys. Rev. D **78**, 114024 (2008).
[66] A. V. Efremov, P. Schweitzer, O. V. Teryaev and P. Zavada, Phys. Rev. D **83**, 054025 (2011); Phys. Rev. D **80**, 014021 (2009).
[67] J. C. Collins, D. E. Soper and G. Sterman, Nucl. Phys. B **250**, 199 (1985).
[68] F. Landry, R. Brock, P. M. Nadolsky and C. P. Yuan, Phys. Rev. D **67**, 073016 (2003).
[69] S. M. Aybat, T. C. Rogers, arXiv:1101.5057 [hep-ph].
[70] L. P. Gamberg *et al.*, Phys. Lett. **B639**, 508-512 (2006).
[71] R. N. Cahn, Phys. Lett. B **78**, 269 (1978).
[72] B. Pasquini, M. Traini and S. Boffi, Phys. Rev. D **71**, 034022 (2005); M. Traini, A. Mair, A. Zambarda and V. Vento, Nucl. Phys. A **614**, 472 (1997).
[73] A. D. Martin, W. J. Stirling, R. S. Thorne and G. Watt, Eur. Phys. J. C **63** (2009) 189.
[74] J. Pumplin, D. R. Stump, J. Huston, H. L. Lai, P. M. Nadolsky and W. K. Tung, JHEP **0207**, 012 (2002).
[75] X. d. Ji, J. P. Ma and F. Yuan, Nucl. Phys. B **652**, 383 (2003).
[76] F. Schlumpf, arXiv:hep-ph/9211255.
[77] Following [72] we worked at NLO to determine the initial scale (12), which offers better numerical stability important at low scales. But in Secs. IV, V we will use the TMDs in a LO treatment. For that we consistently will use the analog to (12) initial scale $\mu_0^{\rm LO} = 420\,{\rm MeV}$ with $\alpha_s^{\rm LO}(\mu_0^2)/(4\pi) = 0.35$, and $\alpha_s^{\rm LO}(M_Z^2) = 0.13939$ with $\Lambda_{\rm LO}^{(3,4,5)} = 359,\ 322,\ 255$ MeV [73]. With these values the LO-value of $\langle x(Q)\rangle_{\rm val} = 0.35$ at 10 GeV^2 is reproduced within numerical accuracy.
[78] F. A. Ceccopieri and L. Trentadue, Phys. Lett. B **636**, 310 (2006); Phys. Lett. B **660**, 43 (2008). F. A. Ceccopieri, Mod. Phys. Lett. **A24**, 3025-3032 (2009).
[79] I. O. Cherednikov and N. G. Stefanis, Phys. Rev. D **80**, 054008 (2009); Phys. Rev. D **77**, 094001 (2008); Nucl. Phys. B **802**, 146 (2008).
[80] Z. B. Kang and J. W. Qiu, Phys. Rev. D **79**, 016003 (2009).
[81] J. Zhou, F. Yuan and Z. T. Liang, Phys. Rev. D **79**, 114022 (2009); W. Vogelsang and F. Yuan, Phys. Rev. D **79**, 094010 (2009).
[82] Besides evolving $f_{1T}^{\perp(1)a}(x)$ according to the non-singlet $f_1^a(x)$-evolution (case (A): solid line in Fig. 2a), we explored also the following LO evolution patterns. (B) non-singlet $g_1^a(x)$-evolution, which is a 'polarized' evolution pattern (as in the Sivers effect), and gives *exactly* the same result as (A) because the evolution kernels coincide. (C) full (including singlet) $f_1^a(x)$-evolution as used in [53]. In the range of applicability of the model for $x > 0.1$, this pattern agrees within 5 % with (A) but it spoils the Burkardt sum rule. The radiatively generated Sivers gluons are moreover not suppressed with respect to Sivers q or $\bar{q}$ distributions, in conflict with the prediction from the limit of a large number of colors N_c, *i.e.* $f_{1T}^{\perp g}/f_{1T}^{\perp q} \sim 1/N_c$ [26]. (D) transversity evolution, the most drastic evolution variation we explored. The chiral-odd evolution pattern decouples from gluons, and avoids conflict with the Burkardt sum rule or the large-N_c limit. For $x > 0.1$ it gives results which are about 20 % smaller than (A). For $h_1^{\perp(1)a}(x)$ we explored the following variations. (E) transversity evolution, solid line in Fig. 2b, which is the evolution pattern of the (p_T-integrated) chiral-odd quark correlator giving rise (if unintegrated) also to $h_1^\perp$. (F) non-singlet $g_1^a(x)$-evolution describing polarized quarks (as $h_1^\perp$) but in a polarized target (in contrast to $h_1^\perp$). (G) non-singlet $f_1^a(x)$-evolution describing unpolarized quarks (in contrast to $h_1^\perp$) though in a unpolarized target (as $h_1^\perp$). The patterns (F) and (G) give identical results, and agree with (E) within 20 %. We are grateful to the referee for stimulating this study.
[83] V. M. Braun, A. N. Manashov and J. Rohrwild, Nucl. Phys. B **826**, 235 (2010).
[84] D. Boer, Nucl. Phys. **B603**, 195-217 (2001).
[85] S. Kretzer, E. Leader, E. Christova, Eur. Phys. J. **C22**, 269-276 (2001).
[86] A. V. Efremov, K. Goeke and P. Schweitzer, Phys. Rev. D **73**, 094025 (2006).
[87] M. Anselmino *et al.*, Phys. Rev. D **75**, 054032 (2007); Nucl. Phys. Proc. Suppl. **191**, 98-107 (2009).
[88] A. Airapetian *et al.* [HERMES Collaboration], Phys. Lett. B **684**, 114 (2010).
[89] J.-F. Rajotte [COMPASS], arXiv:1008.5125 [hep-ex].
[90] In [59] for asymmetries due to chiral-odd TMDs phenomenological parameterizations were used for $f_1^a(x)$, arguing this would tend to reduce model dependence in that case. Whether one uses parameterizations or model results for $f_1^a(x)$ is strictly speaking a higher order effect and in principle within model accuracy. Here we adopt

for both asymmetries $f_1^a(x)$ from the model, which yields a somewhat better description of the data in the case of the Boer-Mulders effect.

[91] A. Airapetian *et al.* [HERMES Collaboration], Phys. Lett. **B693**, 11 (2010).